

## NH<sub>4</sub>Y AND HY ZEOLITES AS ELECTROLYTES IN HYDROGEN SENSORS

M. DEKKER, I. 't ZAND, J. SCHRAM and J. SCHOONMAN

*Laboratory of Inorganic Chemistry, Delft University of Technology, Julianalaan 136, 2628 BL Delft, The Netherlands*

Received 27 July 1988; accepted for publication 24 August 1988

Partly exchanged NH<sub>4</sub>Y and HY zeolites and H<sub>3</sub>O<sup>+</sup>  $\beta/\beta''$ -alumina have been studied as solid electrolyte in a Nernst-type hydrogen sensor. The zeolites were examined on structure using X-ray diffraction and TGA. The electrical properties were studied using impedance spectroscopy. As solid electrode material H<sub>0.34</sub>MoO<sub>3</sub> was investigated. NH<sub>4</sub>Y is a promising material. Response times of a test probe with NH<sub>4</sub>Y as solid electrolyte were less than 8 min. The sensor exhibits excellent Nernst response.

### 1. Introduction

Non-destructive hydrogen sensors are of practical interest because of the importance to detect hydrogen enclosed in construction metals, and in atmospheres in several chemical processes. Nernst-type chemical sensors are attractive because of their selectivity, fast response, and ease of use. Moreover, the probe can be elegantly adapted to the measurement of H<sub>2</sub> in atmospheres (indirect hydrogen activity sensor: IHAS) and hydrogen dissolved in a metal or alloy (direct hydrogen activity sensor: DHAS). In the latter case a direct contact is made between the sample metal and the solid electrolyte.

Several investigations have been reported on materials for use in these probes [1]. As reference electrode PdH<sub>x</sub> [1-4], WO<sub>3</sub> [3,5], PbO<sub>2</sub> [6] and H<sub>x</sub>MoO<sub>3</sub> [4] were tested. As solid electrolyte a variety of materials has been examined, like hydrogen uranyl phosphate (HUP) [1,2,7,8], (Zr(HPO<sub>4</sub>)<sub>2</sub>·nH<sub>2</sub>O) [9], and Nafion, a perfluoro-sulphonic acid resin [3]. Of these, HUP has been studied widely. However, HUP can be used only within a limited temperature range (25-60°C), because dehydration causing the protonic conduction to vanish, occurs at elevated temperatures.

In general, proton conduction is assumed to occur according to two mechanisms, the first being the migration of polyatomic ions like H<sub>3</sub>O<sup>+</sup> or NH<sub>4</sub><sup>+</sup>, and the second one involving proton hopping along "receivers", accompanied by reorientation of these

molecules [10]. Usually the second mechanism is dominating because of its lower activation enthalpy.

This type of conduction is also found in zeolites like HY and NH<sub>4</sub>Y, which can be prepared from NaY by cation exchange up to about 45% HY or NH<sub>4</sub>Y [10]. These compounds exhibit better thermal stability than HUP. In addition, the loss and uptake of H<sub>2</sub>O is at least partially reversible.

The ceramic proton conductor H<sub>3</sub>O<sup>+</sup>  $\beta/\beta''$ -alumina can be made by cation exchange of Na<sup>+</sup>  $\beta/\beta''$ -alumina [11,12]. This material also exhibits good thermal stability.

The present paper deals with the synthesis and characterization of these material using IR spectroscopy, X-ray diffraction, thermo gravimetric analysis (TGA) and atomic emission spectrometry (AES). Conductivity properties are studied using small signal ac response studies in a wide frequency range. The impedance data are fitted to an electrical circuit model description.

The compound H<sub>0.34</sub>MoO<sub>3</sub> was also prepared and structurally characterized for use as solid reference electrode.

Finally a test probe comprising of H<sub>0.34</sub>MoO<sub>3</sub>, NH<sub>4</sub>Y and Pd as the sensing electrode, is examined on its Nernst behaviour and response time in H<sub>2</sub>/N<sub>2</sub> mixtures.

## 2. Experimental

A mixture of about 45%  $\text{NH}_4\text{Y}$  and 55%  $\text{NaY}$  was obtained by exchanging  $\text{NaY}$  (Union Carbide) in 0.1 M  $\text{NH}_4\text{Cl}$  solution for 24 h at room temperature. The partly exchanged  $\text{NaY}$  was washed with water and dried at 50°C.

$\text{HY}$  was obtained by calcining  $\text{NH}_4\text{Y}$  at 450°C for 4.5 h. A heating rate of 1°C/min was used to prevent any possible deformation.

$\text{H}_3\text{O}^+$   $\beta/\beta''$ -alumina was prepared by ion exchange in concentrated  $\text{H}_2\text{SO}_4$  at 300°C for six days.

$\text{H}_{0.34}\text{MoO}_3$  was prepared using the procedure of ref. [13].  $\text{Zn}$  was added to a solution of  $\text{MoO}_3$  in 1.64 M  $\text{HCl}$ . After 24 h the precipitate was washed, and dried over  $\text{P}_2\text{O}_5$ .

IR spectra of  $\text{NH}_4\text{Y}$  and  $\text{HY}$  in  $\text{KBr}$  were recorded. X-ray diffraction ( $\text{Cu K}\alpha$ ) was carried out with all compounds, using a Guinier-de Wolff camera. The TGA measurements were performed on a home-made thermobalance with a commercial temperature controller (Eurotherm). The TGA measurements on the zeolites were made both in water saturated and dry air. Inductively Coupled Plasma AES was carried out on the zeolites with a Perkin Elmer Plasma II.

The electrical properties were studied using impedance spectroscopy in the frequency range 0.1 to 65000 Hz. Here too, a comparison was made as concerning the zeolites between the response in two different ambients, i.e. dry air and water saturated  $\text{N}_2$ . The equipment consisted of a stainless steel conductivity cell provided with resistive heating and two Pt contacts (fig. 1), a Solartron 1250 frequency response analyser and a Solartron 1286 electrochemical interface, coupled to an Olivetti M24 PC. 2-point measurements were performed on pressed pellets of 1 cm in diameter, and about 2 mm thickness, of the solid electrolytes and solid reference electrode. A pressure of 630 MPa was used. Sputtered Pt on both sides served as electrode (Edwards 150B sputter coater).

A software package was developed, involving coordinated data storage, graphical presentation, and a Marquardt non-linear least squares parameter estimation for complex data. With this program the experimental dispersions can be fitted to equivalent circuit descriptions.

$\text{NH}_4\text{Y}$  is measured from room temperature up to

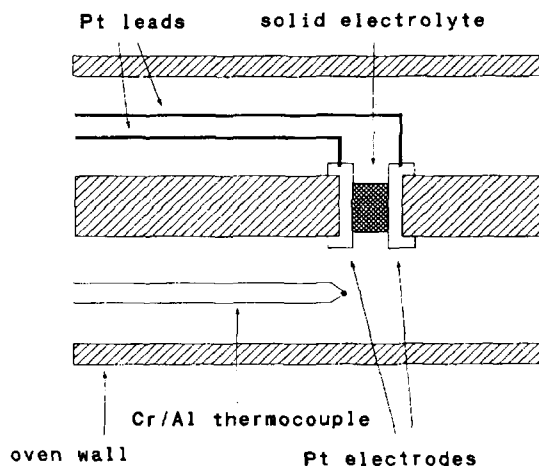


Fig. 1. Measuring cell for impedance spectroscopy.

190°C,  $\text{HY}$  from room temperature up to 350°C, and  $\text{H}_3\text{O}^+$   $\beta/\beta''$ -alumina from room temperature to 250°C.  $\text{H}_{0.34}\text{MoO}_3$  is measured from room temperature up to 100°C.

A sensor was made by pressing together the solid electrolyte  $\text{NH}_4\text{Y}$  or  $\text{HY}$  and the reference electrode material. Two mixtures of both compounds in different proportions were required to obtain a mechanically stable interface. Pd was finally sputtered onto the solid electrolyte as a sensing electrode. The probe was tested in  $\text{H}_2/\text{N}_2$  mixtures as shown in fig. 2. The gases were lead over Pd and Cu catalysts, respectively. The  $\text{NH}_4\text{Y}$  sensor was tested on Nernst behaviour at  $T=28^\circ\text{C}$  and  $T=63^\circ\text{C}$ .

## 3. Results and discussion

The zeolites  $\text{NH}_4\text{Y}$  and  $\text{HY}$  revealed X-ray diffraction patterns which were in good agreement with ASTM reference cards, indicating that the zeolite Y-structure was well conserved during the synthesis. The presence of  $\text{NH}_4^+$  cations in  $\text{NH}_4\text{Y}$  was detected by infrared spectroscopy. An absorption peak at 1400  $\text{cm}^{-1}$  could be assigned to the presence of  $\text{NH}_3$  groups. In  $\text{HY}$  this absorption was absent. The formula of the zeolites is written as



with M denoting  $\text{NH}_4^+$ , respectively,  $\text{H}^+$ . The AES measurements yielded a Si/Al proportion of 2.4 for

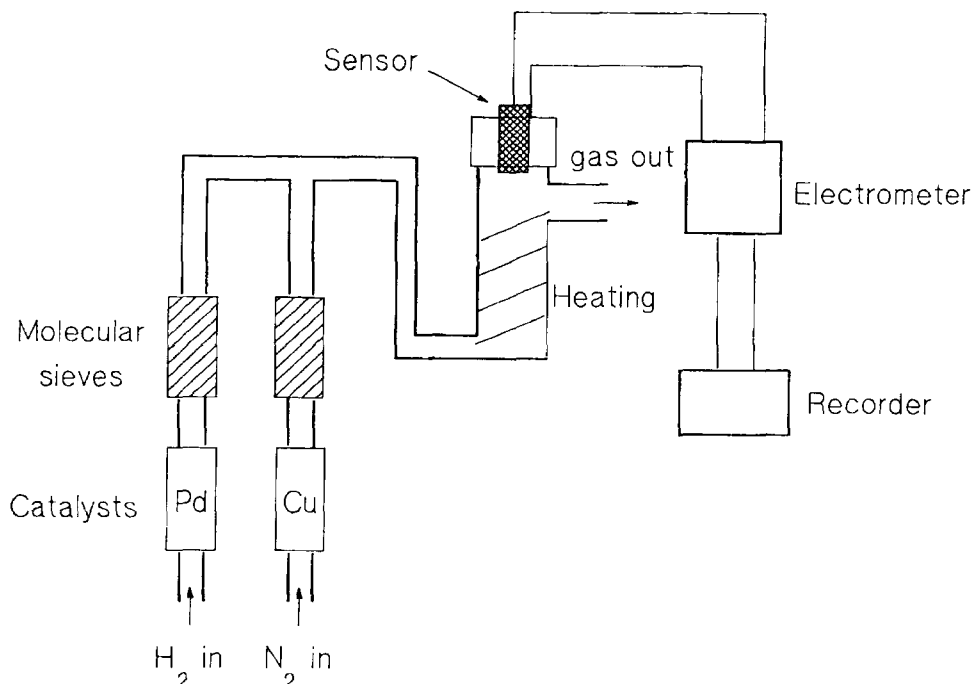


Fig. 2. Schematic of setup for testing a hydrogen sensor.

both compounds, which is in reasonable agreement with these formulae.

Thermogravimetric analyses yielded results shown in fig. 3. Both zeolites appear to lose weight gradually. For  $\text{HY}$  the weight loss occurs in the temperature range  $50\text{--}200^\circ\text{C}$  (water-saturated air), respectively,  $50\text{--}300^\circ\text{C}$  (dry air), while for  $\text{NH}_4\text{Y}$  the range of  $50\text{--}350^\circ\text{C}$  is found to be valid for both ambients. To explain the difference between the two compounds the loss of  $\text{NH}_3$  in  $\text{NH}_4\text{Y}$  beyond  $200^\circ\text{C}$  is of importance [14]. Dehydration may be completed at lower temperatures than  $350^\circ\text{C}$ , followed by  $\text{NH}_3$  loss.  $\text{NH}_3$  constitutes only 3.5 wt% of the dry solid electrolyte, and the weight loss above  $200^\circ\text{C}$  is accordingly small. Another indication for the loss of  $\text{NH}_3$  could be the presence of small but sharp weight decreases above this temperature to be seen in a differential TGA plot (dTGA, fig. 3b), at temperature near  $280^\circ\text{C}$ . These peaks are lacking in the graphs for  $\text{HY}$  (fig. 3d).

The difference in temperature ranges for weight losses of  $\text{HY}$  in dry and water-saturated air indicates an incomplete dehydration of the zeolites in wet at-

mospheres up to  $>300^\circ\text{C}$ . It is well known that complete dehydration of the zeolites leads to an irreversible reorganisation of the structure of the compound. As a consequence conductivity pathways disappear, and hence application as solid electrolyte should be restricted to these temperature limits.

Analyses of the impedance spectra provided bulk conductivities, presented as an Arrhenius plot in fig. 4.  $\text{NH}_4\text{Y}$  turned out to be the better ionic conductor. Bulk conductivities could be determined with our equipment from room temperature onwards. As an upper limit  $200^\circ\text{C}$  was chosen, in concordance with the results of the TGA experiments which indicate the compound to disintegrate above this temperature. The ionic conductivity is increasing up to  $65^\circ\text{C}$  with an activation enthalpy of 0.4 eV in dry air and slightly less in water-saturated nitrogen. The conductivity exceeds that of HUP [2,7]. At low temperatures the conductivity in water saturated  $\text{N}_2$  is much higher than in dry air. The conduction is thus very sensitive to the water content in the environment. Above  $65^\circ\text{C}$ , the influence of the water content of the environment is small, which is in agree-

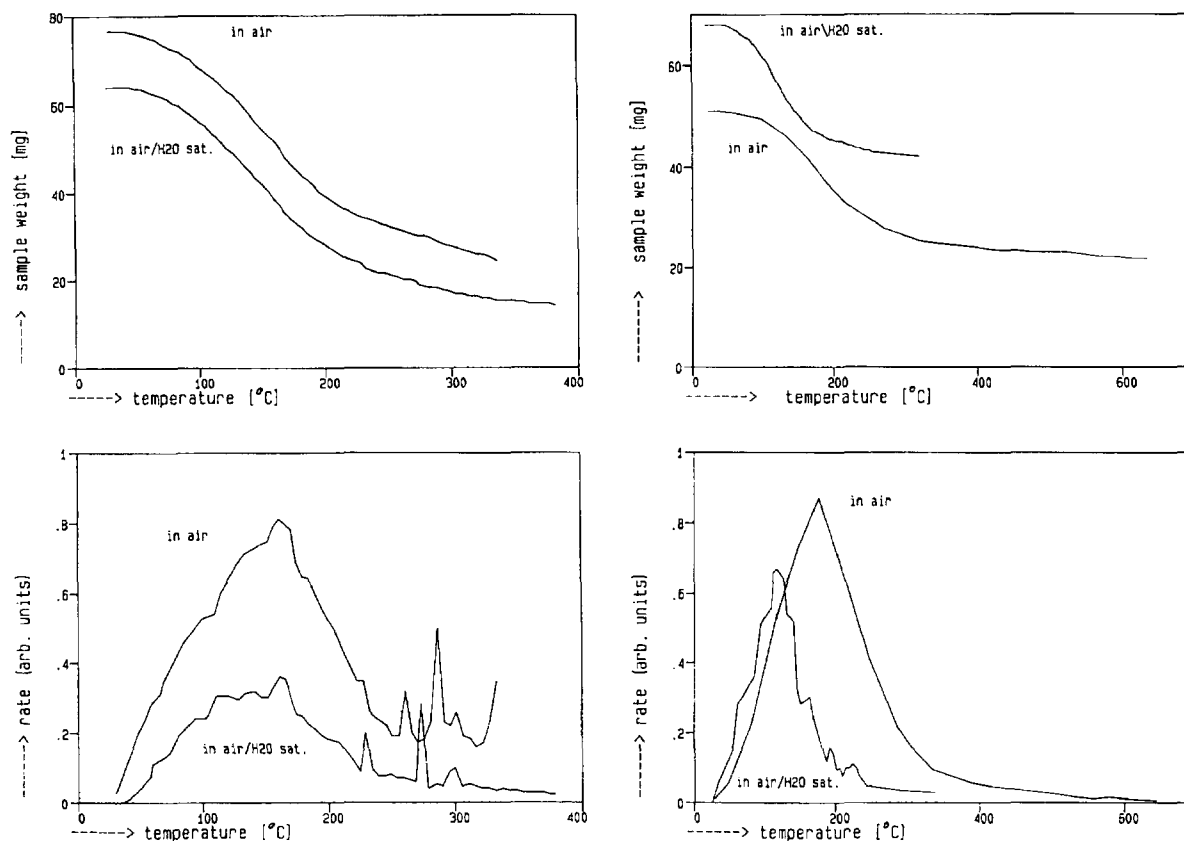


Fig. 3. (a) TGA of  $\text{NH}_4\text{Y}$  in dry and water saturated air respectively; (b) dTGA of  $\text{NH}_4\text{Y}$  in dry water saturated air respectively; (c) TGA and  $\text{HY}$  in dry and water saturated air respectively; (d) dTGA of  $\text{HY}$  in dry and water saturated air respectively.

ment with the TGA spectra. From 65°C onwards dehydration is occurring, and a gradually decreasing conductivity is observed. It is expected however, that the ionic conductivity will increase once more beyond about 250°C, when the structure will become essentially that of  $\text{HY}$ . This however is not relevant for application, because these processes, both complete dehydration and loss of  $\text{NH}_3$ , appeared to be irreversible in our measurements, in agreement with the literature [14]. So  $\text{NH}_4\text{Y}$  may well be applicable up to 200°C.

For  $\text{HY}$  the hypothesis of a smaller loss of water in  $\text{H}_2\text{O}$ -saturated ambients as indicated by the TGA results is supported by the observation that the conductivity increases more rapidly with temperature in a wet ambient than in a dry ambient. Hence a slightly higher conductivity is observed above 250°C. The activation enthalpy above 200°C was in both cases

about 0.7 eV. Below 200°C the dehydration area is characterized by rather unstable bulk conductivities. Only the measurements in air in this range are represented here. The conductivity was much lower than in  $\text{NH}_4\text{Y}$ , and at room temperature the conductance was too low to be detected reliably with the present equipment.

The dispersions of the zeolites were fitted to an equivalent circuit given in fig. 5. An example of a fit for  $\text{NH}_4\text{Y}$  at 127°C is shown in fig. 6. The temperature dependence of the parameters  $R_{gb}$ ,  $Q_{dl}$  and  $Q_g$  for  $\text{NH}_4\text{Y}$  are presented in fig. 7. In the model  $R_b$  denotes the bulk resistance. The constant phase element  $Q_g$  may be associated with geometrical capacitance. The  $\alpha$  value is quite high, indicating the predominant capacitive effects. Below 60°C this element was replaced by a capacitance.  $Q_{dl}$  and  $R_{gb}$  represent interface effects (blocking and diffusion limited con-

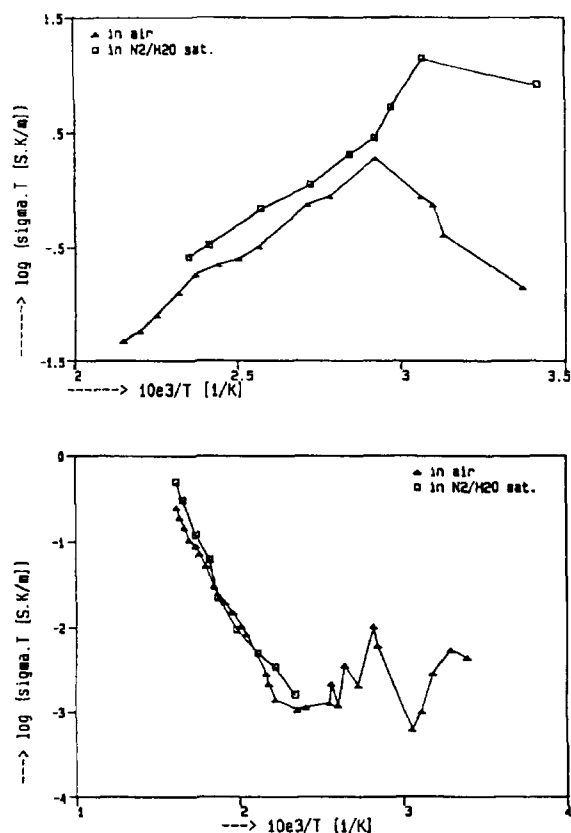


Fig. 4. (a) Arrhenius plot of the bulk conductivity of  $\text{NH}_4\text{Y}$  in dry air and water saturated  $\text{N}_2$  respectively; (b) Arrhenius plot of the bulk conductivity of  $\text{HY}$  in dry air and water saturated  $\text{N}_2$  respectively.

ductance) and grain boundary resistance, respectively.  $R_{gb}$  is decreasing with temperature. Hence it is improbable that this quantity can be assigned to a surface conductance which might be present at low temperatures, but merely with grain boundary effects within the structure. The interface effects are not strongly dependent on temperature. Most of the fits show less than 12% relative error, and from the smooth temperature dependence of the parameters involved one may conclude that one conductance mechanism dominates in the whole temperature range. The highest temperatures could indicate a change, but these points are too few in number to base any conclusion on.

Concerning  $\text{H}_3\text{O}^+ \beta/\beta''$ -alumina no references X-ray data seem to exist. The pattern recorded here re-

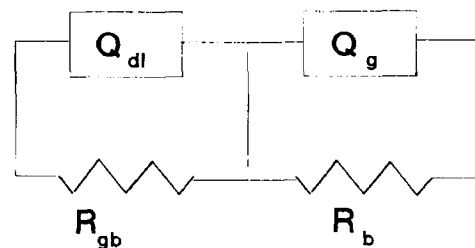


Fig. 5. Equivalent circuit used to fit the dispersions of  $\text{NH}_4\text{Y}$ .

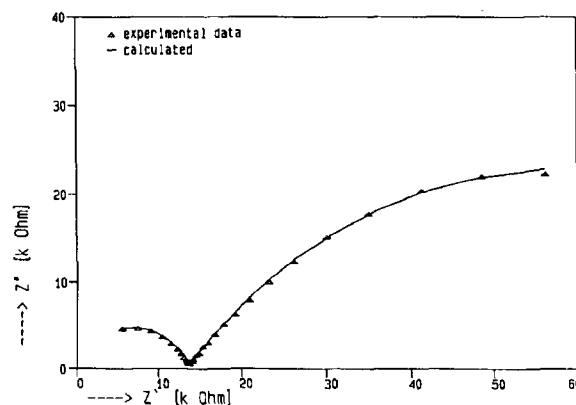


Fig. 6. Example of a non linear least squares fit:  $\text{NH}_4\text{Y}$  in dry air at  $127^\circ\text{C}$ .

vealed strong reflections at 5.75, 3.46, 2.88, 2.64 and  $2.58 \text{ \AA}$  spacing, and moderate intensity lines at 4.19, 3.51, 2.18, 2.02, 1.73, 1.64 and  $1.415 \text{ \AA}$  spacing.

Differential TGA revealed two peaks at about  $110^\circ\text{C}$  and  $260^\circ\text{C}$ , respectively (fig. 8). The high temperature peak can be ascribed to dehydration as has been reported in the literature [11]. The low temperature peak is ascribed to  $\text{H}_2\text{O}$  loss in the surface areas of the grains.

The conductivity of our materials appeared to be in the order of  $10^{-5} \text{ S/m}$ . Hence it was not tested in a sensor.

The X-ray pattern of  $\text{H}_{0.34}\text{MoO}_3$  revealed the material to be amorphous. This need not be a problem for the use as an electrode as long as a well-fixed hydrogen activity can be established at the interface electrode/electrolyte. TGA measurements showed one peak at about  $100^\circ\text{C}$ . Impedance spectra revealed a rather complex behaviour (fig. 9). As in the case of  $\text{H}_3\text{O}^+ \beta/\beta''$ -alumina, the impedance spectra were not fitted to an equivalent circuit.

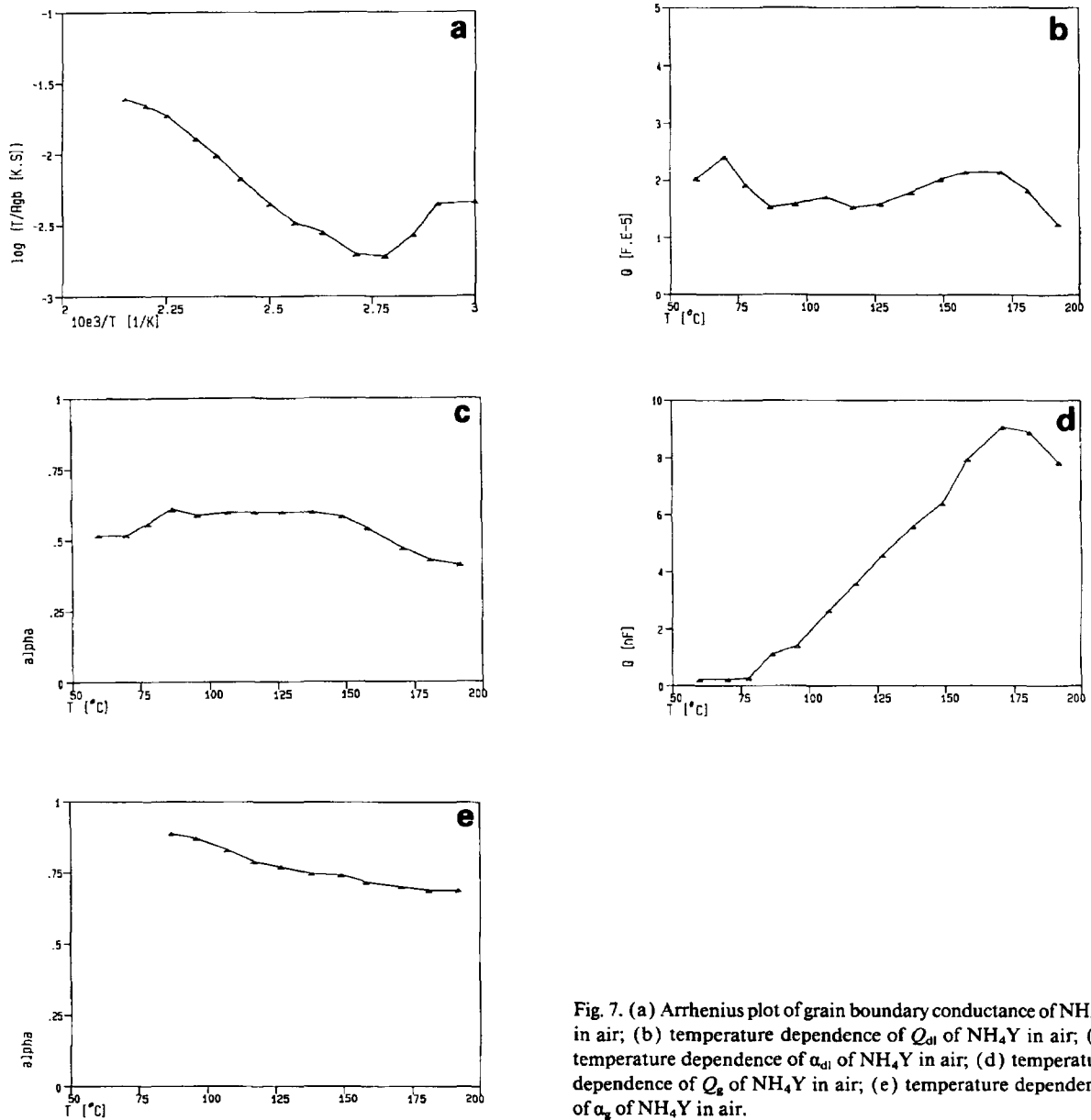


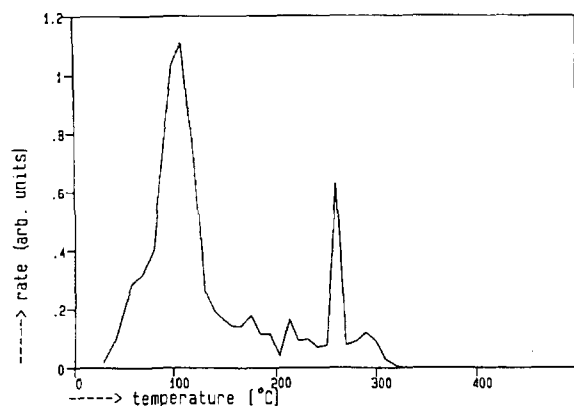
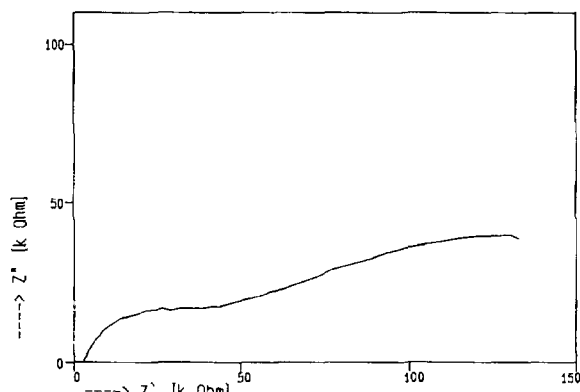
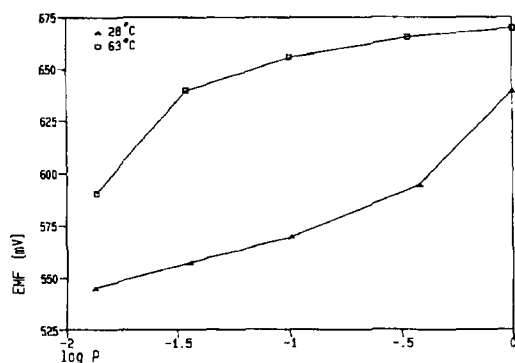
Fig. 7. (a) Arrhenius plot of grain boundary conductance of  $\text{NH}_4\text{Y}$  in air; (b) temperature dependence of  $Q_{dl}$  of  $\text{NH}_4\text{Y}$  in air; (c) temperature dependence of  $\alpha_{dl}$  of  $\text{NH}_4\text{Y}$  in air; (d) temperature dependence of  $Q_s$  of  $\text{NH}_4\text{Y}$  in air; (e) temperature dependence of  $\alpha_s$  of  $\text{NH}_4\text{Y}$  in air.

The sensor prototype has been tested on Nernst behaviour in the range from 0 to 100 mole%  $\text{H}_2$  in  $\text{N}_2$  and response time. Assuming the hydrogen activity at the reference electrode to be constant, the Nernst formula for the cell is

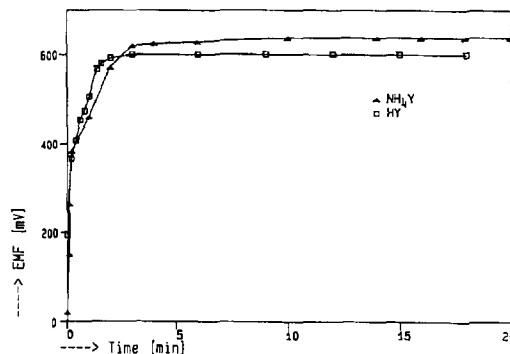
$$E = \Delta E_0 + 2.303 \frac{RT}{nF} \log a_{\text{H}} \quad (2)$$

giving a slope of 0.030 V at  $T=28^\circ\text{C}$  and 0.033 V at  $T=63^\circ\text{C}$ . The response showed excellent agreement with theory at both temperatures (fig. 10). The experimental slopes were 0.031 at  $28^\circ\text{C}$ , and 0.030 at  $64^\circ\text{C}$ . Measurements at higher temperatures will be done in the future.

Response times were all found between two and eight minutes. Some preliminary experiments with

Fig. 8. dTGA of  $\text{H}_3\text{O}^+$   $\beta/\beta'$ -alumina in air.Fig. 9. Example of a dispersion of  $\text{H}_{0.34}\text{MoO}_3$  in air at  $60^\circ\text{C}$ .Fig. 10. Dependence of the EMF on  $P_{\text{H}_2}$  of a probe consisting of  $\text{H}_{0.34}\text{MoO}_3$ ,  $\text{NH}_4\text{Y}$  and hydrated Pd, at 28 and  $63^\circ\text{C}$  respectively.

a sensor using HY as an electrolyte yielded faster response times, even at low temperatures. An example is given in fig. 11.

Fig. 11. Response times at  $28^\circ\text{C}$  with solid electrolyte  $\text{NH}_4\text{Y}$  and HY respectively.

#### 4. Conclusions

$\text{NH}_4\text{Y}$  zeolite is a promising candidate for use as a solid electrolyte in hydrogen sensors. Its protonic conductivity is higher than HUP, and the applicable temperature range is wider ( $20$ – $200^\circ\text{C}$ ). In addition, the zeolite HY could be useful between  $150$  and  $250^\circ\text{C}$ , its conductivity being high enough in this temperature region. In the ranges of application the zeolites do not undergo any discontinuity concerning structure and conductance mechanism. In combination with amorphous  $\text{H}_{0.34}\text{MoO}_3$  as solid reference electrode and  $\text{PdH}_x$  as sensing electrode, a Nernst response can be achieved at least up to  $65^\circ\text{C}$ . The response time of the sensor prototype is relatively short.

#### Acknowledgement

The authors are indebted to Mr. J.F. van Lent for carrying out X-ray diffraction measurements, to Mr. J.J. Tiggelaar for performing the ICP-AES measurements, and to Dr. Ir. G. Hakvoort for the use of the TGA equipment.

#### References

- [1] J. Schoonman, J.L. de Roo, C.W. de Kreuk, and A. Mackor, in: Proc. 2nd Intern. Meeting on Chemical Sensors, Bordeaux, France, 1986, eds. J.-L. Aucouturier, J.S. Cauhopé, M. Destriau, P. Hagenmüller, C. Lucat, F. Ménéil, J. Portier and J. Salardienne (1986) p. 319.

- [2] J. Schoonman, D.R. Franceschetti and J.W. Hanneken, *Ber. Bunsenges. Physik Chem.* 86 (1982) 701.
- [3] D.R. Franceschetti, S.I. Shefsky and J.W. Hanneken, *Int. Adv. Nondestructive Testing* 10 (1984) 101.
- [4] C.W. de Kreuk, J. Schoonman and A. Mackor, in: *Proc. Int. Workshop on Electrochemical Corrosion Testing*, Ferrara, Italy, eds. E. Heitz, J.C. Rowlands and F. Mansfeld (1985) p. 53.
- [5] S.B. Lyon and D.J. Fray, *Br. Corros. J.* 19 (1984) 23.
- [6] R.V. Kumar and D.J. Fray, *Proc. 2nd Intern. Meeting on Chemical Sensors*, Bordeaux, France 1986, eds. J.L. Aucouturier, J.S. Cauhopé, M. Destriau, P. Hagenmuller, C. Lucat, F. Ménil, J. Portier and J. Salardienne, p. 306.
- [7] J. Schoonman and H.S. Kiliaan, *Solid State Ionics* 9/10 (1983) 1087.
- [8] M.G. Shilton and A.T. Howe, *Mat. Res. Bull.* 12 (1977) 701.
- [9] N. Miura, H. Kato, N. Yamazoe and T. Seiyama, *Chem. Letters* (1983) 1573.
- [10] S. Yde-Andersen, E. Skou, I.G. Krogh Andersen and E. Krogh Andersen, in: *Solid State Protonic Conductors III*, eds. J.B. Goodenough, J.J. Jensen and A. Potier (Odense University Press, Odense, 1985) p. 247.
- [11] G.C. Farrington and J.L. Briant, *Mat. Res. Bull.* 13 (1978) 763.
- [12] P.S. Nicholson, M.Z.A. Munshi, G. Singh, M. Sayer and M.F. Bell, *Solid State Ionics* 18/19 (1986) 699.
- [13] O. Glemser and G. Lutz, *Z. Anorg. Allg. Chem.* 264 (1951) 17.
- [14] G.T. Kerr and A.W. Chester, *Thermochim. Acta* 3 (1971) 113.